Journal of Molecular Structure 890 (2008) 90–94

Contents lists available at ScienceDirect

Journal of Molecular Structure

journal homepage: www.elsevier.com/locate/molstruc

N,*N*′-Dimethylbenzamidine and derivatives: Preparations, structures, and hydrogen bond networks therein

Wei-Zhong Chen, Guo-Lin Xu, Conrad G. Jablonski, Tong Ren *

Department of Chemistry, Purdue University, 560 Oval Drive, West Lafayette, IN 4790, USA

ARTICLE INFO

Article history:
Received 13 December 2007
Received in revised form 12 March 2008
Accepted 12 March 2008
Available online 21 March 2008

Dedicated to the memory of Professor Al Cotton

Keywords:
Benzamidine
Hydrogen bonding
Crystal structures

ABSTRACT

Reported herein are the syntheses of *N*,*N*′-dimethylbenzamidine (HDMBA, **1**) and its phenyl substituted derivatives HYDMBA with phenyl substituents *Y* as 3-CH_3O (**2**), and 3-CF_3 (**3**), and the determination of single crystal structures of compounds **1**–**3**. In addition, the crystal structures of the salts of **1** with HBF_4 (**1a**), oxalic acid (**1b**), terephthalic acid (**1c**), and **2** with HCl (**2d**) are also reported. Interesting configurations and H-bonding patterns due to the orientation of two methyl groups were observed.

1. Introduction

Ligands containing amidine group have played important roles in both coordination and organometallic chemistry [1–3]. Frequently utilized amidine ligands include *N*,*N*′-diarylformamidines (HDArF), 2-anilinopyrdines (Hap), guanidines, and benzamidines, as shown in Chart 1. The DArF ligands have been used extensively to support both the transition metal and main group metal complexes [2,4], especially as the bridging ligand in bimetallic paddlewheel motifs [5]. In addition, amidinates have also found applications such as ancillary ligands for Ziegler-Natta catalysts [6] and molecular precursors for ALD (atomic layer deposition) [7]. The strong electron donor nature of amidinates also renders a unique redox richness of the resultant complexes. In an extreme case, $W_2(hpp)_4$ (Hhpp = 1,3,4,6,7,8-hexahydro-2*H*-pyrimido[1,2-*a*]pyrimidine) was found to be more electropositive than Cs metal [8].

A major focus area in our laboratory is to use the diruthenium alkynyl compounds supported by amidinates including DArF and ap (Chart 1) as the building blocks of molecular wires and molecular devices [9]. Our particular interest in *N*,*N*′-dialkylbenzamidinates is rooted in their ability to support paddlewheel dinuclear transition metal compounds without hindering axial ligation, which was first demonstrated by Cotton and coworkers with the synthesis of $Cr_2(DMBA)_4$ and $Re_2(DMBA)_4Cl_2$ (DMBA = *N*,*N*′-dimethylbenzamidinate) [10]. A series of diruthenium compounds supported by *N*,*N*′-dialkylbenzamidinate have been prepared and become valuable platforms for both the exploration of charge mobility along metal-alkynyl backbone and the building blocks of molecular wires and molecular diodes [11]. *N*,*N*′-Dialkylbenzamidine with bulky alkyl groups such as ^{i}Pr, ^{t}Bu, and cyclohexyl can be readily prepared from the reactions between an appropriate carbodiimide (RN═C═NR) and alkyl lithium (LiR′). Such an easy preparation is unavailable for homolog of smaller R such as methyl and ethyl because of the instability of the corresponding carbodiimides. Described in this contribution are the synthesis of *N*,*N*′-dimethylbenzamidine (HDMBA) and its phenyl-substituted derivatives (Chart 2), their crystal structures and intermolecular hydrogen bonding patterns therein.

2. Results and discussion

2.1. Syntheses

N,*N*′-Dimethylbenzamidine (**1**) was synthesized from *N*-methylbenzamide in two steps (Scheme 1) with an overall yield of ca. 40% using a procedure slightly modified from that in the literature [12]. The same procedure was used for the preparation of compounds **2** and **3**, where appropriately substituted *N*-methylbenzamides were used and yields were between 40% and 80%. The salts of amidines with various acids, as defined in Table 1, were generated in methanol solutions and crystallized upon the introduction of ether via vapor diffusion.

* Corresponding author. Tel.: +1 765 494 5466; fax: +1 765 494 0239.
E-mail address: tren@purdue.edu (T. Ren).

0022-2860/$ - see front matter © 2008 Elsevier B.V. All rights reserved.
doi:10.1016/j.molstruc.2008.03.018

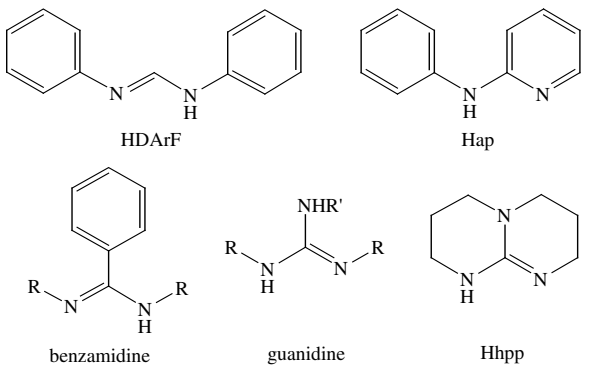

Chart 1. Common amidines.

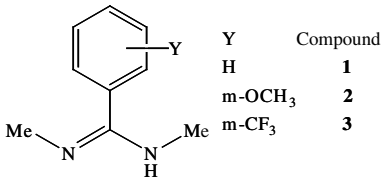

Chart 2. HDMBA and derivatives.

2.2. Crystal structures

The structures of compounds **1**, **2**, **3**, **1a**, **1b**, **1c**, and **2d** were determined through single crystal X-ray diffraction studies, and the respective ORTEP plots including one packing diagram for **1** are shown in Figs. 1–8. The amidine group of all neutral compounds **1**–**3** adopts the same *E,Z*-configuration, where the amino (designated as N1) *N*-methyl group is *trans*- to the C_{ipso} (C4) center and the imino (N2) *N*-methyl group is *cis*- to the C_{ipso} center.

The amino hydrogen (H1) was located from the difference map in each of **1**–**3** and successfully refined, which confirms a localized N1—H1 bond. Among the neutral compounds, two C—N bonds can be unambiguously assigned as amino C—N bond (C1—N1, 1.349–1.353 Å) and imino C—N double bond (C1—N2, 1.268–1.297 Å) on the basis of bond lengths. Limited literature precedents of the HDMBA-type structures include those of *N,N′*-dimethyl-4-nitrobenzamidine [13] and *N,N′*-dimethyl-4-halobenzamidine (halogen = Br and I) [14], where the configurations of amidine group are identical to those of compounds **1**–**3** [13].

Neutral compounds **1**–**3** engage zig-zag intermolecular hydrogen bonding in the crystalline state. As illustrated by Fig. 4 for crystal **1**, compounds **1**–**3** form a one-dimensional H-bonding chain in solid state, where the amino H center interacts with the imino N center from the adjacent molecule. The formation of the same type 1D H-bonding chain should be expected for *N,N′*-dimethyl-4-nitrobenzamidine, except that the coordinate of the amino hydrogen was not reported in that structure [13]. The hydrogen bonding pattern of HDMBA compounds also contradicts the patterns observed for HDArF and Hap, where the head-to-tail dimer is predominant (see Chart 3) [3,15].

Compounds **1**–**3** can be readily protonated by both strong and weak protic acids, and the resultant ions form aggregates primarily via the formation of one or several salt bridges. The protonation of

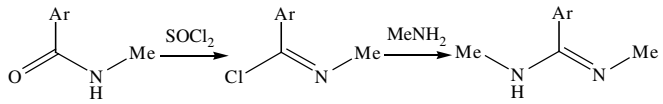

Scheme 1. Synthesis of HDMBA.

Table 1
Salts formed between amidine and acid (ratio, designation)

	HBF_4	Oxalic	Terephthalic	HCl
1	1:1, **1a**	1:2, **1b**	3:4, **1c**	–
2	–	–	–	1:1, **2d**

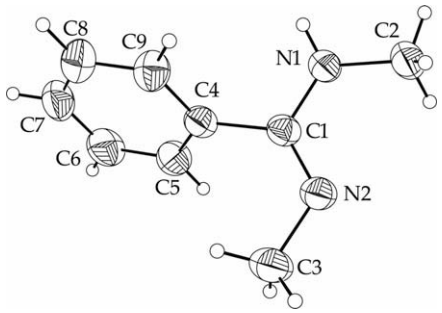

Fig. 1. ORTEP plot of molecule **1** at 30% probability level. Selected bond lengths (Å) and angles (°): C1—N1, 1.351(2); C1—N2, 1.282(2); C1—C4, 1.494(2); N1—C1—N2, 120.0(2).

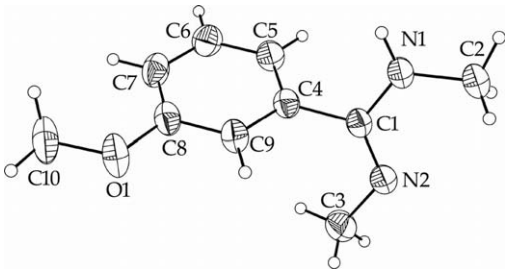

Fig. 2. ORTEP plot of molecule **2** at 30% probability level. Selected bond lengths (Å) and angles (°): C1—N1, 1.345(2); C1—N2, 1.280(2); C1—C4, 1.500(2); N1—C1—N2, 120.5(2).

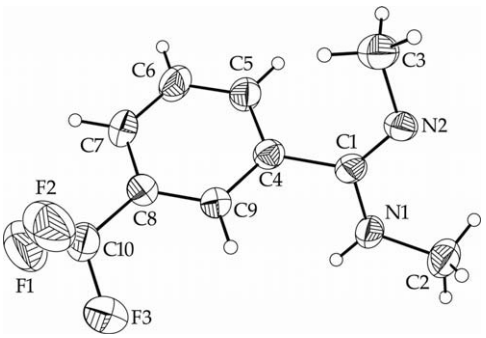

Fig. 3. ORTEP plot of molecule **3** at 30% probability level. Selected bond lengths (Å) and angles (°): C1—N1, 1.349(4); C1—N2, 1.268(3); C1—C4, 1.508(4); N1—C1—N2, 120.8(3).

compound **1** by HBF_4 resulted in compound **1a**, and its crystal structure is shown in Fig. 5. As shown in Fig. 5, both of the N-bound hydrogen atoms were located from the difference map and successfully refined, and each interacts with a BF_4^-. Notably, the C1—N1 (1.304(6) Å) and C1—N2 (1.312(6) Å) bond lengths are identical within the experimental errors, indicating that the positive charge is delocalized over the entire amidinium unit. Thus, each N—H···BF_4^- pair accounts for one half of the salt bridge. Two F atoms from each BF_4^- are involved in the salt bridge, which led to a one-dimension chain of ion-pairs.

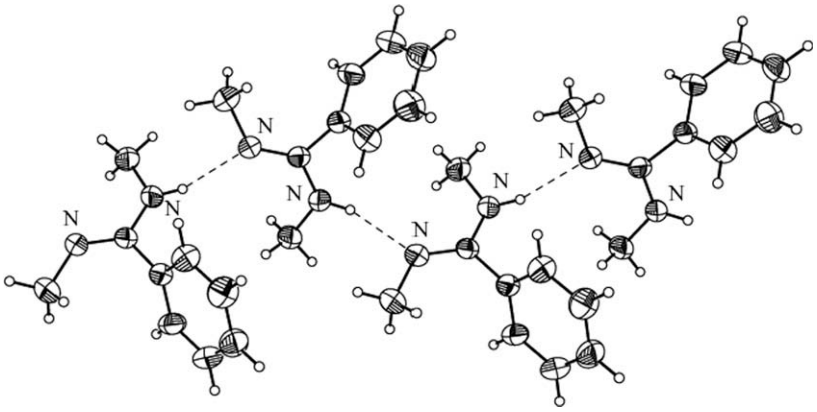

Fig. 4. Intermolecular H-bonding diagram of molecule **1**.

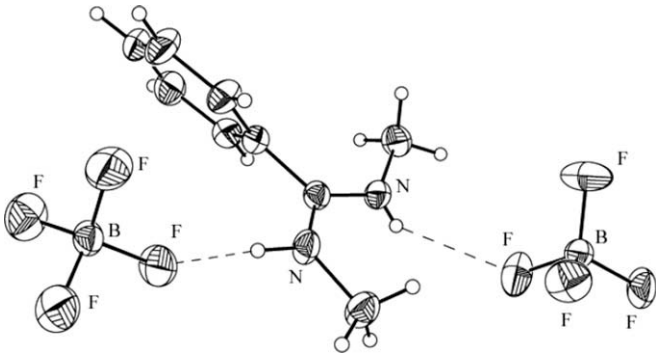

Fig. 5. H-bonding diagram of molecule **1a**.

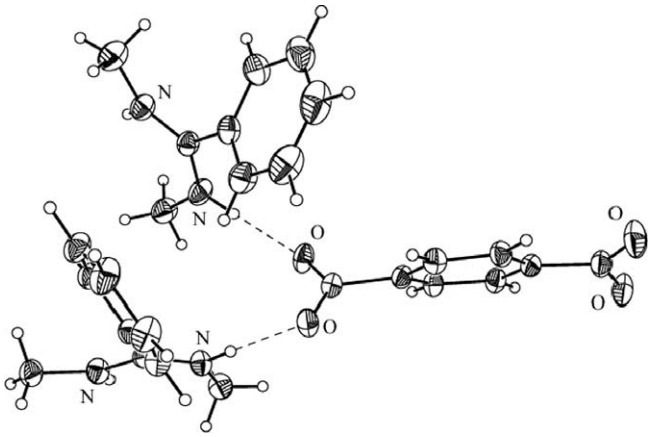

Fig. 7. Simplified H-bonding diagram of molecule **1c**.

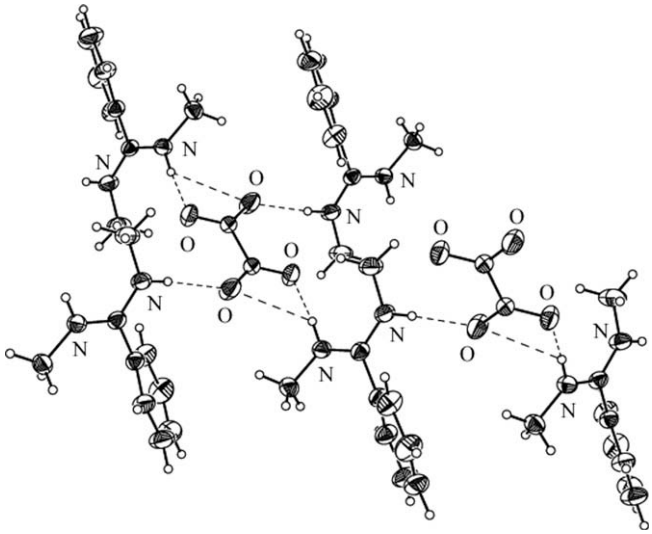

Fig. 6. Simplified H-bonding diagram of molecule **1b**.

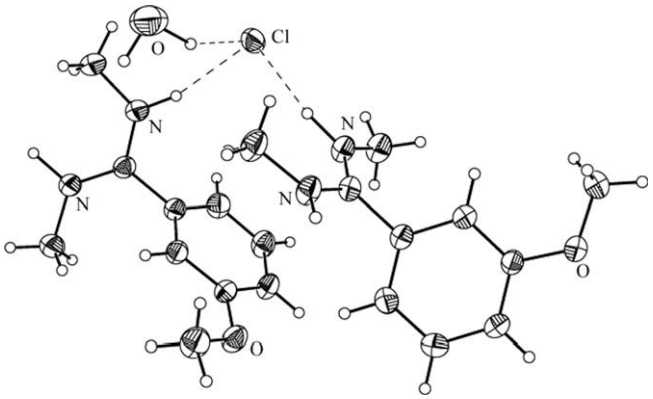

Fig. 8. H-bonding diagram of molecule **2d**.

The co-crystallization of compound **1** with oxalic acid resulted in a salt $[H\cdot\mathbf{1}]_2$(oxalate) (**1b**). The asymmetric unit of **1b** contains one $[H\mathbf{1}]^+$ and one half of an oxalate, and an inversion center bisects the oxalate. Similar to **1a**, both of the N-bound hydrogen atoms were located and refined, and a delocalized amidinium unit was implicated by the equal C—N bond lengths. The oxalate oxygen centers engage hydrogen bonding with one or two $[H\mathbf{1}]^+$, which results in a 2D H-bonding network shown in Fig. 6. A 2:1 salt, $[H\cdot\mathbf{1}]_2$(terephthalate) (**1c**, Fig. 7), was formed when **1** was co-crystallized with terephthalic acid. In addition to a unit of $[H\cdot\mathbf{1}]_2$(terephthalate), the asymmetric unit of **1c** contains one half of a free terephthalic acid molecule. More intricate 3D network was formed through various salt bridges between $H\mathbf{1}^+$ and terephthalate, while free terephthalic acids form a linear chain through hydrogen bonding. Previously, the salt bridge formation was described for the pair of *N*,*N*′-diethylbenzamidine and ferrocenecarboxylic acid, where hydrogen bonding interaction is limited within the pair [16].

Crystal **2d** is a HCl salt of compound **2**, and the asymmetric unit contains one unit of [H**2**]Cl and a water molecule. As shown in Fig. 8, the chloride interacts with three different H centers: one hydrogen from water and two hydrogens from different amidinium groups, and the latter interactions resulted in a one-dimensional chain of salt bridges.

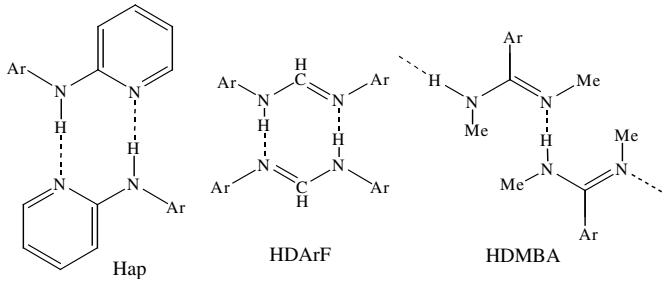

Chart 3. Hydrogen bonding patterns in amidines.

3. Conclusion

Our results revealed that the amidine group in *N*,*N*′-dimethylbenzamidines adopt an *E*,*Z*-configuration, which results in a 1D zig-zag hydrogen bonding chain. Upon protonation, the salt bridges between amidinium and anion also result in various extended networks.

4. Experimental

4.1. General

Benzoyl chloride, 3-methoxylbenzoic acid, 4-bromobenzoyl chloride, terephthalic acid, thionyl chloride were purchased from ACROS, 3-trifluoromethylbenzoic acid was purchased from OAKWOOD, and methylamine hydrochloride was purchased from Aldrich. Synthesis of *N*,*N*′-dimethylbenzamidine (**1**) was modified from that of the literature [12], and some detailed description is given below. ^{1}H and ^{13}C NMR spectra were recorded on a Bruker AVANCE300 NMR spectrometer, with chemical shifts (δ) referenced to the residual $CHCl_3$ and the solvent $CDCl_3$, respectively. Infrared spectra were recorded on a Perkin-Elmer 2000 FT-IR spectrometer using KBr disks.

4.2. Preparation of *1*

A 100 mL round-bottomed flask was charged with 20 g of *N*-methylbenzamide (prepared from the treatment of benzoyl chloride with methylamine in water) and 20 mL thionyl chloride. The mixture was heated to reflux until the cease of gas evolution from the reaction mixture (about 2 h). The excess thionyl chloride was distilled off under a reduced pressure and the residue was further distilled under reduced pressure (ca. 0.1 torr) to yield a colorless liquid (14 g, 61%). The distilled product from the preceding reaction was added dropwise to a 50 mL aqueous methylamine solution (generated in situ from 18 g of methylamine hydrochloride with 11 g of NaOH in water) in 20 min at 0 °C. The resultant mixture was warmed to room temperature and stirred for another 3 h. The mixture was then treated with NaOH (aq) and extracted with CH_2Cl_2 (3 × 50 mL). The organic layer was collected and the solvent was removed by rotavapor to yield a sticky solid. Further recrystallization from CH_2Cl_2 and hexanes gave a pure white solid (10 g, 71.4%). Data for **1**: ^{1}H NMR: 7.29–7.27 (*m*, 3H, aromatic), 7.16–7.14 (*m*, 2H, aromatic), 4.18 (*s*, 1H, N*H*), 2.77 (*s*, 6H, NCH_3); ^{13}C NMR: 161.5, 135.8, 129.2, 128.8, 127.9, 27.0; MS-FAB (*m*/*e*): 147 [M^+−H]; IR (υ/cm^{-1}): 3205, 2938, 1629, 1540, 1402, 1336, 1158, 1038, 1003, 915, 774, 701.

4.3. Preparation of *2*

N,*N*′-Dimethyl-3-methoxyl-benzamidine (**2**) was prepared in 65% yield using the same procedure as that of **1** from *N*-methyl-3-methoxyl-benzamide instead of *N*-methylbenzamide. Data for **2**: ^{1}H NMR: 7.26–7.21 (*m*, 1H, aromatic), 6.84–6.70 (*m*, 3H, aromatic), 4.17 (*s*, 1H, N*H*), 3.73 (*s*, 3H, OCH_3), 2.79 (*s*, 6H, NCH_3); ^{13}C NMR: 161.2, 159.9, 137.3, 129.9, 120.2, 114.8, 113.4, 55.7; MS-FAB (*m*/*e*): 179 [M+H]; IR (υ/cm^{-1}): 3196, 2928, 1623, 1558, 1404, 1337, 1140, 1050, 1013, 892, 787, 715.

4.4. Preparation of *3*

N,*N*′-Dimethyl-3-trifloromethyl-benzamidine (**3**) was prepared in 46% yield using the same procedure as that for **1** from *N*-methyl-3-trifluoromethyl-benzamide instead of *N*-methylbenzamide. Data for **3**: ^{1}H NMR: 7.51–7.42 (*m*, 4H, aromatic), 4.15 (*s*, 1H, N*H*), 2.86 (*s*, 6H, NCH_3); ^{13}C NMR: 167.2, 159.7, 136.7, 131.6, 129.4, 126.1, 124.9, 122.4, 27.2; MS-FAB (*m*/*e*): 215 [M^+−H]; IR (υ/cm^{-1}): 3205, 2943, 1629, 1558, 1406, 1329, 1167, 1071, 907, 809, 704.

4.5. X-ray data collection, processing, and structure analysis and refinement

Single crystals of **1**–**3**, were grown via either diffusion of hexanes into a CH_2Cl_2 solution (**1**) or slow evaporation of hexanes/CH_2Cl_2 solutions (**2** and **3**). Salts **1a**, **1b**, **1c**, and **2d** were prepared by dissolving appropriate amidine and acid with ethanol in a small vial, which was then enclosed in a larger vial containing ether. Crystals suitable for X-ray diffraction study were harvested after 24 h. The X-ray intensity data were measured at 300 K on a Bruker SMART1000 CCD-based X-ray diffractometer system using MoKα

Table 2
Crystallographic data for compounds **1**, **1a**–**c**, **2**, **2d**, and **3**

	1	**2**	**3**	**1a**	**1b**	**1c**	**2d**
Formula	$C_9H_{12}N_2$	$C_{10}H_{14}N_2O$	$C_{10}H_{11}F_3N_2$	$C_9H_{13}N_2$ BF_4	$C_{20}H_{26}N_4O_4$	$C_{30}H_{33}N_4O_6$	$C_{10}H_{17}ClN_2O_2$
FW	148.21	178.23	216.21	236.02	386.45	545.60	232.71
Space group	*Pbca*	*Pbca*	$P2_1/c$	$P2_1/n$	$P2_1/n$	$P2_1/c$	$P2_1/c$
a (Å)	8.6624(6)	8.3555(8)	9.228(2)	10.662(2)	9.0756(5)	9.6208(7)	11.4889(7)
b (Å)	11.3426(8)	8.4040(7)	13.411(3)	7.726(1)	9.9715(6)	19.308(1)	10.4510(7)
c (Å)	18.391(1)	29.080(3)	8.622(2)	13.732(2)	11.4323(7)	15.340(1)	10.9843(7)
β (°)	90	90	98.356(5)	90.507(3)	95.931(1)	94.229(1)	111.722(2)
V (Å^3)	1807.0(2)	2042.0(3)	1055.7(4)	1131.1(3)	1029.1(1)	2841.7(4)	1225.24(1)
Z	8	8	4	4	2	4	4
T (°C)	27	27	27	27	27	27	27
λ (MoKα) (Å)	0.71073	0.71073	0.71073	0.71073	0.71073	0.71073	0.71073
ρ_{calc} (g cm^{-3})	1.09	1.160	1.360	1.386	1.247	1.275	1.262
μ (mm−1)	0.075	0.077	0.120	0.129	0.088	0.090	0.296
R_1 ($I > 2\sigma$ (I))	0.040	0.042	0.059	0.097	0.044	0.048	0.040
wR_2 ($I > 2\sigma$ (I))	0.110	0.111	0.129	0.334	0.120	0.136	0.116
GOF	1.01	1.05	0.83	1.01	1.01	1.01	1.05

(λ = 0.71073 Å). Crystals used for X-ray crystallographic analysis were cemented onto a quartz fiber with epoxy glue. Data were measured using omega scans of 0.3° per frame such that a hemisphere (1271 frames) was collected. No decay was indicated for any of four data sets by the recollection of the first 50 frames at the end of each data collection. The frames were integrated with the Bruker SAINT© software package [17] using a narrow-frame integration algorithm, which also corrects for the Lorentz and polarization effects. Absorption corrections were applied using SADABS supplied by George Sheldrick.

The structures were solved and refined using the Bruker SHELXTL© (Version 5.1) software package [18] in the space groups *P*bca, *P*bca, $P2_1/c$, $P2_1/n$, $P2_1/n$, $P2_1/c$, and $P2_1/c$ for crystals **1**, **2**, **3**, **1a**, **1b**, **1c**, and **2d**, respectively. Positions of all non-hydrogen atoms and the *N*-hydrogen were located by the direct method. With all non-hydrogen atoms being anisotropic and all hydrogen atoms except *N*-hydrogen in calculated position and riding mode the structure was refined to convergence by least squares method on F^2, SHELXL-93, incorporated in SHELXTL.PC V 5.03 [18] (Table 2).

5. Supporting Information available

Crystallographic data for the structural analysis have been deposited with the Cambridge Crystallographic Data Center, CCDC 670438–670443 for compounds **1**, **1a**–**c**, **2**, **2d**, and **3**, respectively. Copies of this information may be obtained free of charge from, The Director, CCDC, 12 Union Road, Cambridge CB2 1EZ, UK, (Fax: +44 1233 336033; email: deposit@ccdc.cam.ac.uk or www: http://ccdc.cam.ac.uk).

Acknowledgement

This work is supported by the National Science Foundation (Grants Nos. CHE 0242623/0553564 and CHE 0715404).

References

[1] F.T. Edelmann, Coord. Chem. Rev. 137 (1994) 403;
P.J. Bailey, S. Pace, Coord. Chem. Rev. 214 (2001) 91.
[2] J. Barker, M. Kilner, Coord. Chem. Rev. 133 (1994) 219.
[3] M.P. Coles, Dalton Trans. (2006) 985.
[4] P.C. Junk, M.L. Cole, Chem. Commun. (2007) 1579;
M.L. Cole, D.J. Evans, P.C. Junk, M.K. Smith, Chem. Eur. J. 9 (2003) 415;
G.B. Deacon, C.M. Forsyth, P.C. Junk, J. Wang, Inorg. Chem. 46 (2007) 10022.
[5] F.A. Cotton, C.A. Murillo, R.A. Walton (Eds.), Multiple Bonds between Metal Atoms, Third ed., Springer Science and Business Media, Inc., New York, 2005;
F.A. Cotton, C. Lin, C.A. Murillo, Acc. Chem. Res. 34 (2001) 759;
T. Ren, Coord. Chem. Rev. 175 (1998) 43;
C. Lin, J.D. Protasiewicz, E.T. Smith, T. Ren, J. Chem. Soc., Chem. Commun. (1995) 2257;
C. Lin, J.D. Protasiewicz, E.T. Smith, T. Ren, Inorg. Chem. 35 (1996) 6422;
Z.K. Chan, T.R. Chen, Y.F. Tsai, J.D. Chen, J.C. Wang, Polyhedron 26 (2007) 3715;
Y.Y. Wu, Y.C. Kao, J.D. Chen, C.H. Hung, Inorg. Chim. Acta 357 (2004) 1002.
[6] K.C. Jayaratne, L.R. Sita, J. Am. Chem. Soc. 122 (2000) 958;
A. Littke, N. Sleiman, C. Bensimon, D.S. Richeson, G.P.A. Yap, S.J. Brown, Organometallics 17 (1998) 446.
[7] Z. Li, S.T. Barry, R.G. Gordon, Inorg. Chem. 44 (2005) 1728;
A.R. Sadique, M.J. Heeg, C.H. Winter, Inorg. Chem. 40 (2001) 6349.
[8] F.A. Cotton, N.E. Gruhn, J. Gu, P. Huang, D.L. Lichtenberger, C.A. Murillo, L.O.V. Dorn, C.C. Wilkinson, Science 298 (2002) 1971.
[9] T. Ren, Organometallics 24 (2005) 4854;
S.K. Hurst, T. Ren, J. Organomet. Chem. 670 (2003) 188;
T. Ren, G.-L. Xu, Comments Inorg. Chem. 23 (2002) 355.
[10] A. Bino, F.A. Cotton, W. Kaim, Inorg. Chem. 18 (1979) 3566;
F.A. Cotton, W.H. Ilsley, W. Kaim, Inorg. Chem. 19 (1980) 2360.
[11] G. Xu, C. Campana, T. Ren, Inorg. Chem. 41 (2002) 3521;
S.K. Hurst, G.-L. Xu, T. Ren, Organometallics 22 (2003) 4118;
G.-L. Xu, C.G. Jablonski, T. Ren, Inorg. Chim. Acta 343 (2003) 387;
G.-L. Xu, C.G. Jablonski, T. Ren, J. Organomet. Chem. 683 (2003) 388;
G.-L. Xu, M.C. DeRosa, R.J. Crutchley, T. Ren, J. Am. Chem. Soc. 126 (2004) 3728;
G.-L. Xu, R.J. Crutchley, M.C. DeRosa, Q.-J. Pan, H.-X. Zhang, X. Wang, T. Ren, J. Am. Chem. Soc. 127 (2005) 13354;
J.-W. Ying, D.R. Sobransingh, G.-L. Xu, A.E. Kaifer, T. Ren, Chem. Commun. (2005) 357;
J.-W. Ying, T. Ren, J. Organomet. Chem. 691 (2006) 4021;
J.-W. Ying, A. Cordova, T.Y. Ren, G.-L. Xu, T. Ren, Chem. Eur. J. 13 (2007) 6874.
[12] S.J. Angyal, W.K. Warburton, Aust. J. Sci. Res. 4 (1951) 93.
[13] B. Tinant, J.P. Declercq, J. Podlaha, O. Exner, Collect. Czech. Chem. Commun. 54 (1989) 3245.
[14] W. Chen, T. Ren, J. Cluster Sci. 19 (2008) 99.
[15] R. Anulewicz, I. Wawer, T.M. Krygowski, F. Mannle, H.H. Limbach, J. Am. Chem. Soc. 119 (1997) 12223;
T. Ren, S. Radak, Y.-H. Ni, G.-L. Xu, C. Lin, K.L. Shaffer, V. DeSilva, J. Chem. Crystallogr. 32 (2002) 197;
G.-L. Xu, A. Cordova, T. Ren, J. Cluster Sci. 15 (2004) 413;
B. Xi, G.-L. Xu, J.-W. Ying, H.-L. Han, A. Cordova, T. Ren, J. Organomet. Chem 693 (2008) 1656.
[16] G. Cooke, F.M.A. Duclairoir, A. Kraft, G. Rosair, V.M. Rotello, Tetrahedron Lett. 45 (2007) 557.
[17] SAINT V 6.035 Software for the CCD Detector System, Bruker-AXS Inc., 1999.
[18] SHELXTL 5.03 (WINDOW-NT Version), Program Library for Structure Solution and Molecular Graphics, 1998, Bruker-AXS Inc.; SHELXL-93, Program for the Refinement of Crystal Structures, University of Göttigen, Germany, 1993.